

THE LAWRENCE BERKELEY LABORATORY GEOTHERMAL  
PROGRAM IN NORTHERN NEVADA\*

Kenneth F. Mirk and Harold A. Wollenberg  
Lawrence Berkeley Laboratory  
University of California  
Berkeley, California

The Lawrence Berkeley Laboratory's geothermal program began with consideration of regions where fluids in the temperature range of 150 to 230°C may be economically accessible. Three valleys, located in an area of high regional heat flow in north central Nevada, were selected for geological, geophysical, and geochemical field studies. The objective of these ongoing field activities is to select a site for a 10-MW demonstration plant. Field activities (which started in September 1973) are described. A parallel effort has been directed toward the conceptual design of a 10-MW isobutane binary plant which is planned for construction at the selected site. Design details of the plant are described. Project schedule with milestones is shown together with a cost summary of the project.

## I. INTRODUCTION

The goal of the LBL-UCB geothermal project is to locate, design, and construct a 10-MW (electrical) geothermal pilot demonstration plant, utilizing the low salinity, high-temperature (170-220°C) waters of the northern Great Basin. Concurrently, parameters indicative of such a resource are evaluated by traditional and new geologic, geochemical, and geophysical techniques.

## II. LOCATION

The area chosen for the studies, north-central Nevada, is characterized by higher than normal regional heat flow (Ref. 1). Temperatures at depth in some hot spring systems, determined by chemical geothermometers (Ref. 2), exceed 150-170°C. Figure 1 shows the distribution of heat flow in the western U.S., and the region of high heat flow in northern Nevada. Three sites within this region, Buffalo Valley southwest of Battle Mountain, Grass Valley south of Winnemucca, and Buena Vista Valley southwest of Winnemucca are our present centers of activity. These sites, indicated on the location map (Fig. 2), are all essentially on federal land, and each contains an active hot spring system

---

\*Work done under the auspices of the U.S. Atomic Energy Commission.

(Buffalo Valley Hot Springs, Leach Hot Springs in Grass Valley, and Kyle Hot Springs in Buena Vista Valley).

### III. GEOLOGIC SETTING

Active hot spring areas and potential geothermal resource sites in the Great Basin are in almost all cases associated with steeply dipping basin-and-range faults (Ref. 3), often at the intersections of two major orientations of faulting. This is exemplified in Whirlwind Valley (Fig. 3), where the ENE-trending Malpais escarpment is intersected by a nearly north-south trending fault zone just to the east of the active Beowawe Hot Springs and their accompanying blowing geothermal wells. The fault zones furnish permeable pathways for downward percolating, meteoric water to reach sufficient depth (4 to 5 km) in a region of high geothermal gradient (40 to 60°C/km). The water is heated, then rises on the upward-flowing limb of a convection cell (Fig. 4). Thus, fracture permeability, afforded by intersecting faults in sub-alluvial bedrock, is the mechanism by which waters can reach depths great enough for heating, and provides channelways for upward transport of hot waters. Geothermal reservoirs may be in fractured rock of fault zones, or in relatively permeable beds of Tertiary sedimentary deposits and Quaternary valley fill alluvium.

### IV. FIELD ACTIVITIES

Our site evaluation program combines interrelating geologic, geophysical, and geochemical studies. Interpretation of high-, middle-, and low-altitude aerial photography (much of it provided by NASA), together with surface geologic mapping, disclose the geologic structure of the areas. This information is used to orient geophysical traverses and interpret their results. Concurrently, sampling of country rock and hot-and-cold spring waters, and their subsequent analyses by x-ray fluorescence and neutron activation techniques yield major- and trace-element contents. Information from the geological, geophysical, and geochemical activities is combined to locate several 100- to 150-m deep heat flow holes in each of the areas under study. Results of the heat flow measurements will, in turn, strongly influence the locations of one or more deep test wells (1.5 to 2 km), which may furnish the fluid for a preliminary heat-exchanger test facility.

#### A. Geologic Methods

Because much of the area is in valley fill alluvium, reconnaissance and detail mapping relies heavily on the aforementioned aerial photography. High-altitude (65,000 ft) flights by NASA U-2 aircraft provide regional coverage of high-resolution black and white photographs at low sun angles (Fig. 3 is an example), enhancing fault-related features on the desert floor. Lower-altitude (6,000 ft above surface) color photography at higher sun angles shows detail associated with faulting on the immediate site areas. A structural map of the Leach Hot Springs area, compiled from aerial photography and surface observations, is shown as Fig. 5. Airborne infrared imagery, obtained in predawn

hours, indicates well the known hot spring areas, as well as disclosing a hitherto unknown warm-spring area in the west portion of Buffalo Valley playa.

Mapping and age dating of ancient hydrothermal manifestations and related volcanic rocks in the Leach Hot Springs area and the East Range suggest that these silicified zones, 14 to 16 million years old, are residues of hydrothermal systems that produced many precious metal deposits in northern Nevada (Ref. 4).

## B. Geophysical Methods

Geophysical techniques used, or planned to be used in evaluation of the sites, are listed on Table 1. Of these, electrical resistivity methods have been employed most heavily to date in our site evaluations. An example of results of a bipole-dipole resistivity reconnaissance in Buffalo Valley is shown on Fig. 6. With the current transmitter at the location in Fig. 6, voltages measured throughout the valley furnished a rather featureless apparent resistivity map, with lowest values associated with electrically conductive playa deposits, and higher resistivities with the nearer-surface and exposed bedrock. A similar pattern was obtained with the current dipole at a different location and reoccupation of the voltage measurement points. A dipole-dipole traverse of the valley yielded the vertical profile pseudosection of resistivity and the accompanying model shown on Fig. 7. The resistivity model matches the gravity profile and schematic model constructed by Grannell (Ref. 5) for the same region. Good concordance has been observed between telluric, self-potential, and dipole-dipole resistivity traverses in the strongly faulted area near Leach Hot Springs. In contrast to the Buffalo Valley pattern, order-of-magnitude differences in resistivity over short distances, indicating, most likely, the presence of warm waters, are apparent at Leach. Magnetotelluric and telluric measurements were made along resistivity profile lines crossing Buffalo Valley with good agreement between results of these methods.

Microearthquake activity was monitored by an eight-station seismometer array for several weeks at each of the three sites. Preliminary results indicate appreciable activity southwest of Leach Hot Springs in and surrounding a mid-valley graben zone. The region encompassing the sites was monitored by a broader array, confirming the locus of activity at Leach, as well as an active zone on the east flank of the Tobin Range.

Three preliminary heat flow holes have been drilled in Buffalo Valley. One is within the thermal anomaly surrounding the hot springs, delimited by Olmsted, et al. (1974, private communication); the others are well outside the anomaly to establish the background heat flow of the area and to compare it with heat flows previously measured by the USGS in nearby bedrock terranes (Ref. 1).

A radiometric survey was made of these and other hot spring systems in northern and central Nevada (Ref. 6). Several hot spring systems where calcium carbonate is the predominant deposit exhibit relatively high radioactivities, caused by emanating radon-222. Spring systems where SiO<sub>2</sub> strongly predominates as the deposit material are low in radioactivity. An array of

radon alpha-track detectors was installed within and surrounding the radioactive spring area in Buffalo Valley (Ref. 7). Away from the springs, integrated track densities are greatest in thin alluvium, covering the relatively high radioactivity rhyolitic Fish Creek Mountains Tuff, attesting to emanation of radon from the Tuff through the alluvium. The greatest alpha-track densities are in detectors placed closest to the obviously radioactive pools and mounds in the hot springs area.

### C. Geochemical Methods

Knowledge of major- and trace-element contents of hot and cold spring waters and country rocks within site areas is important for chemical geothermometry, as well as for the study of interactions of rock with hydrothermal waters. Major element abundancies, determined by the nondispersive x-ray fluorescence method (Ref. 8), provide input for temperature estimates based on silica and alkali element ratios. SiO<sub>2</sub> contents of hot and cold spring waters are used in models (Ref. 9) to determine the degree of mixing of near-surface cold water with rising hydrothermal water. Neutron activation analyses of trace elements (Ref. 10) in waters and rocks may provide "fingerprints" of the rocks through which the waters passed, illuminating their pathways from their source area into and within the geothermal system. Furthermore, knowledge of water chemistry is necessary for plant design, and for evaluation of environmental impact of the development of the geothermal resource.

### V. 10-MW PILOT PLANT

In January 1974 a program was initiated at Berkeley to develop a conceptual design for a 10-MW pilot plant to be located at the Nevada site. The primary objective of this design study was to produce a realistic cost estimate and schedule for overall program planning. This study was completed in June of this year and reviewed by Rogers Engineering of San Francisco, the architect and engineering firm selected by the AEC for this initial engineering phase. A brief summary of the results of this design study follows.

Prior to starting the final design study these assumptions were made:

- (1) A binary power cycle.
- (2) Isobutane as the working fluid.
- (3) A wellhead brine temperature of 200°C.
- (4) Brine salinity < 3000 ppm total dissolved solids.

A simplified flow schematic is presented in Fig. 8. Three production wells (each with an output of 375,000 lb/hr) and two reinjection wells are required. Each production well is equipped with a downhole pump to provide sufficient pressure head to the brine to prevent flashing and keep any dissolved CO<sub>2</sub> in solution. Temperature of brine exiting the last heat exchanger section is 235°F, and the entire mass flow of  $1.1 \times 10^6$  lb/hr is reinjected. A single

brine/isobutane heat exchanger is indicated on the schematic; the actual plant will contain eight shell- and tube-type units connected in series. Each unit has a shell diameter of 5 ft and a tube length of 20 ft. The units are so manifolded that any pair can be isolated for cleaning without interrupting the operation of the remaining units. For cost estimating purposes 304L stainless-steel tubes are assumed, and an overall heat transfer coefficient of approximately  $100 \text{ Btu/ft}^2 \times \text{hr} \times \text{deg F}$  is used.

An isobutane condensate temperature of  $100^\circ\text{F}$  is assumed, resulting in a hot well pressure of 72 psia. Two condensate feed pumps are included in the design. Each pump is driven by a separate isobutane turbine. In addition to the main feed pumps, a smaller electrically driven feed pump (not shown on schematic) is provided for start-up purposes. The feed pumps supply sufficient head to allow the system to operate in the super critical region. This is done to minimize the "pinch-point" effect in the brine/isobutane exchanger.

A regenerative heat exchanger is included in the design. The purpose of this exchanger is to remove the large amount of superheat contained in the exhaust of the turbines and to transfer this heat to the feed isobutane.

Isobutane vapor leaving the brine/isobutane exchanger is directed to both the main and feed pump turbines. A pressure of 600 psia is maintained at the main turbine inlet by controlling the speed of the feed pump turbines. Brine flow through the main heat exchanger is regulated to maintain a turbine inlet temperature of  $370^\circ\text{F}$ . Two types of turbines were considered: an axial flow reaction unit and a radial inflow reaction unit. The radial inflow unit was selected for this conceptual design. This particular turbine is a single-stage unit having an impeller diameter of 23 in. and rotates at 9000 rpm, necessitating a reduction unit between the turbine and generator. The turbo-generator unit is rated at 10 MW; plant auxiliaries consume 2 MW, resulting in a net plant output of 8 MW. Exhaust vapor from the turbines passes through the other half of the regenerative exchanger, where it is cooled about  $140^\circ\text{F}$  prior to entering the condenser.

The condenser is located in a dry-type cooling tower. Both wet- and dry-type towers were considered. A dry-type tower results in a higher initial cost and a somewhat lower plant efficiency due to the large fan power requirements. However, both maintenance and environmental problems are greatly reduced with the use of a dry-type tower, and for these reasons this type was selected. A dry-bulb temperature of  $80^\circ\text{F}$  is assumed for design study purposes. Condensate returns by gravity from condenser section to the hot well.

Not shown on the schematic is an automatic control system whose design allows the plant to be operated from a remote station located anywhere within the distribution system. All plant operations, with the exception of initial startup, can be performed by this system.

The general arrangement of the various plant components is illustrated in Fig. 9. The three production wells are shown in the background with the main brine pipeline terminating at the eight brine/isobutane heat exchangers located in the foreground. The two reinjection wells are not shown on the pictorial but are located to the viewer's right. In order to provide sufficient head to satisfy

the NPSH requirements of the feed pumps, the condensing section of the cooling tower is elevated. Dimensions of the cooling tower are approximately 100 ft wide by 200 ft long.

The main turbo-generator unit is housed in the building directly to the left of the cooling tower. A 36-in. -diameter line is provided to carry the turbine exhaust to the six regenerative heat exchangers located between the turbo-generator building and the cooling tower. An electrical switchgear yard is shown in the far left corner of the site. Across from the switchyard is a small water storage pond having a surface area of 7200 ft<sup>2</sup> and a storage capacity of 270,000 gal. The pond is used to furnish auxiliary cooling for small heat loads, such as the generator lube oil system, and to provide fire protection for the installation. Adjacent to the cooling pond is a test pad where research and development work can be carried out under actual field conditions on plant components such as heat exchangers, expanders, and pumps. The entire plant facility as shown occupies approximately five acres.

A cost estimate summary is presented in Fig. 10. The first six items were estimated by Rogers Engineering and essentially represent the cost of the power plant. The item "Isobutane System" includes the brine/isobutane heat exchangers, regenerative exchanger, instrumentation and controls, plus all the isobutane piping. "Turbine/Generator" includes the feed pumps and their drivers. The cost of the main condenser is included in the "Cooling Tower" cost. "Production/Reinjection Wells" includes the cost of the downhole pumps. Escalation was calculated at 12% per year for a period of 2-1/2 years. A contingency of approximately 22% based on the escalated cost has been included.

The overall project schedule and logic is shown in Fig. 11. The diagram is self-explanatory and, therefore, little comment is required. Final site selection is scheduled for the end of 1975, at which time the final engineering phase of the project will start. A production and reinjection well drilling program will be started in 1976 and completed by the middle of 1977. Plant components will be fabricated in 1977 and installed and tested in the first half of 1978. Start-up operations are scheduled for the third quarter of 1978.

## REFERENCES

1. Sass, J.H., Lachenbruch, A.H., Munroe, R.J., Green, G.W., and Moses, T.H., Jr., "Heat Flow in the Western United States," J. Geophys. Res., Vol. 76, pp. 6376 - 6413, 1971.
2. Mariner, R.H., Rapp, J.B., Willey, L.M., and Presser, T.S., "The Chemical Composition and Estimated Minimum Thermal Reservoir Temperatures of the Principal Hot Springs of Northern and Central Nevada," U.S. Geological Survey open file report, 1974.
3. Hose, R.K., and Taylor, B.E., "Geothermal Systems of Northern Nevada," abstract, Geol. Soc. of Amer. Cordilleran Section 70th Annual Meeting, 1974.
4. Noble, D.C., Wollenberg, H.A., Archibald, D., and Silberman, M., "Cenozoic Structural, Volcanic, and Hydrothermal History of the Leach Hot Springs Geothermal Area, Pershing County, Nevada," abstract submitted to Geol. Soc. of Amer. Cordilleran Section 71st Annual Meeting, 1975.
5. Grannel, R.B., "A Regional Gravity Survey of the Fish Creek Mountains and Surrounding Area, North-Central Nevada," abstract, Geol. Soc. of Amer. Cordilleran Section 70th Annual Meeting, 1974.
6. Wollenberg, H.A., "Radioactivity of Northern Nevada Hot Spring Systems," Geophys. Res. Lett., LBL-2482, 1974 (in press).
7. Wollenberg, H.A., "Radon Alpha-Track Survey of a Potential Geothermal Resource Area," LBL Report, 1974 (in preparation).
8. Hebert, A., and Street, K., "Non-dispersive Soft X-ray Fluorescence Spectrometer for Quantitative Analysis of the Major Elements in Rocks and Minerals," Anal. Chem., Vol. 46, pp. 203, 1974.
9. Fournier, R.O., and Truesdell, A.H., "Geochemical Indicators of Sub-surface Temperature, Part II: Estimation of Temperature and Fraction of Hot Water Mixed with Cold Water," U.S. Geol. Sur. J. Res. - Vol. 2, No. 3, 1974.
10. Bowman, H., Hebert, A., Wollenberg, H., and Asaro, F., "A Detailed Chemical and Radiometric Study of Geothermal Waters and Associated Rock Formations, With Environmental Implications," LBL-2966, 1974.

Table 1. Geophysical methods

---

Deep resistivity	Heat flow
Magnetotellurics	Airborne multispectral
Tellurics	Radiometric
Electromagnetics	Gravity
Microearthquakes	Magnetics
Seismic noise	

---



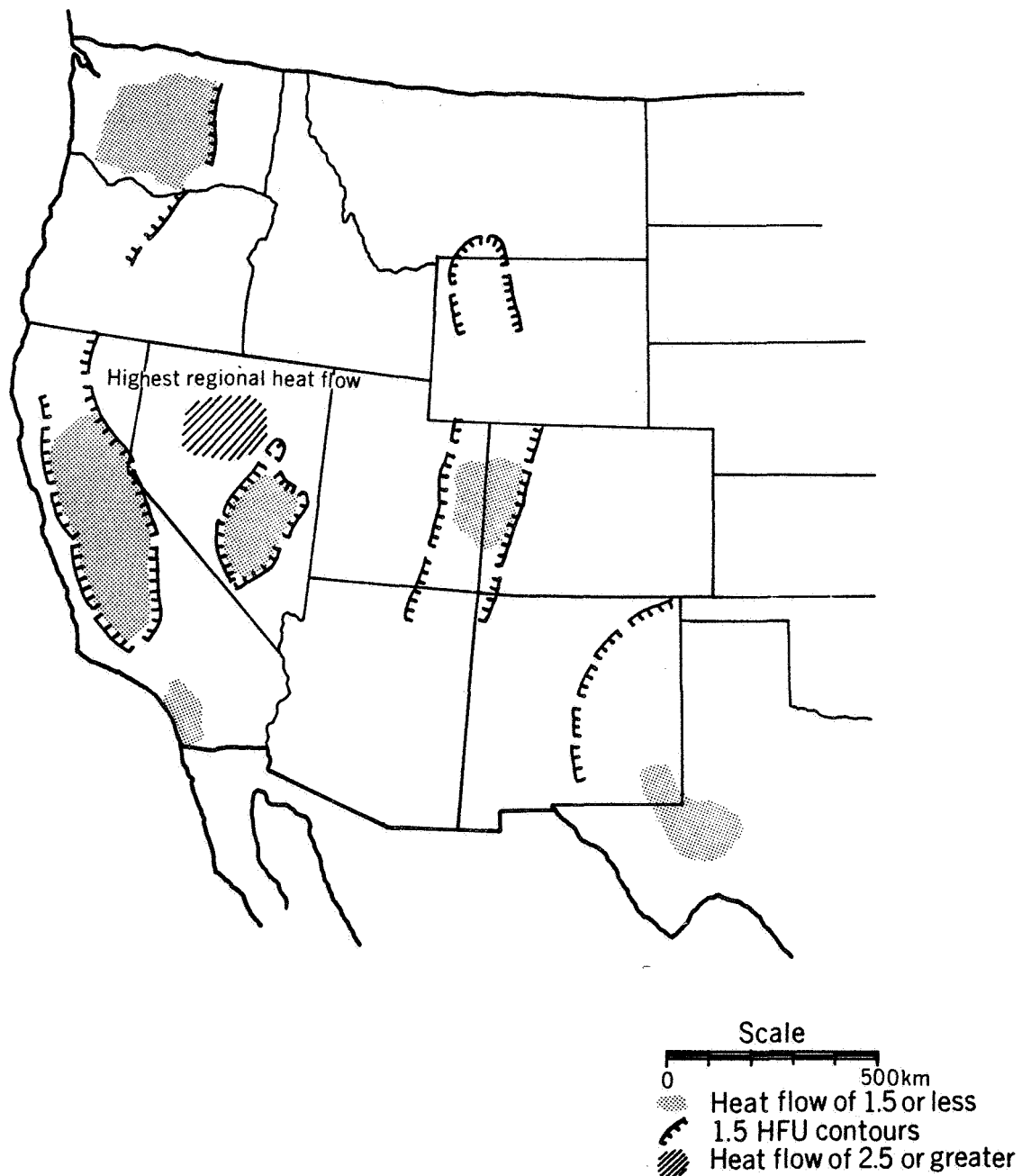
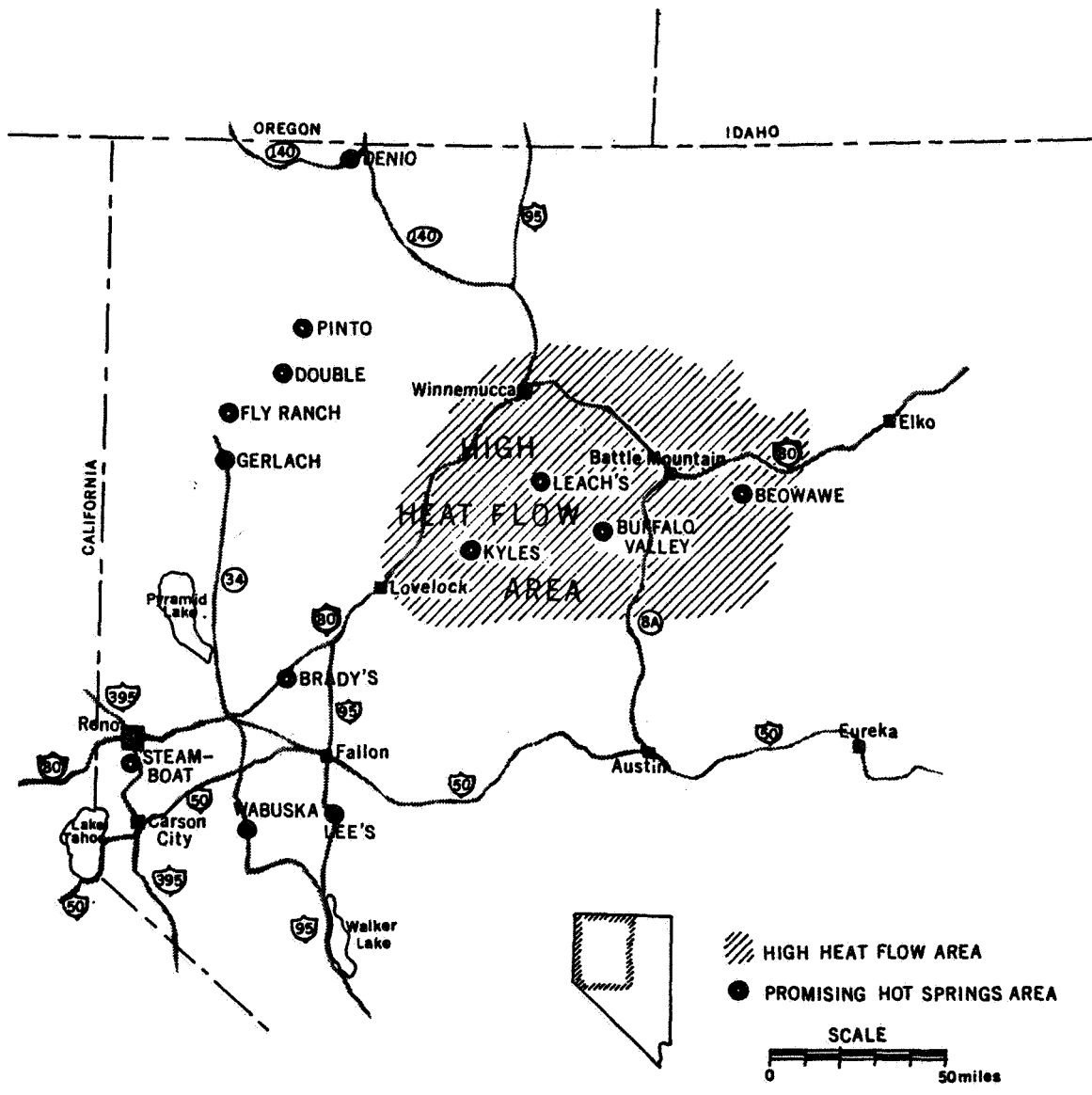


Fig. 1. Regional heat flow in the western U.S. (Ref. 1). The stippled areas have heat flows estimated less than  $1.5 \mu\text{cal}\cdot\text{cm}^{-1}\cdot\text{sec}^{-1}$  (HFU), while in the dashed area, the "Battle Mountain High" heat flow probably exceeds 2.5 HFU. Hachured lines indicate the fairly well-defined position of the 1.5-HFU contour.



## Hot Springs in Northwestern Nevada

XBL 735 676

Fig. 2. Location map, northwestern Nevada, showing prominent thermal spring areas within and outside of the Battle Mountain High heat flow region

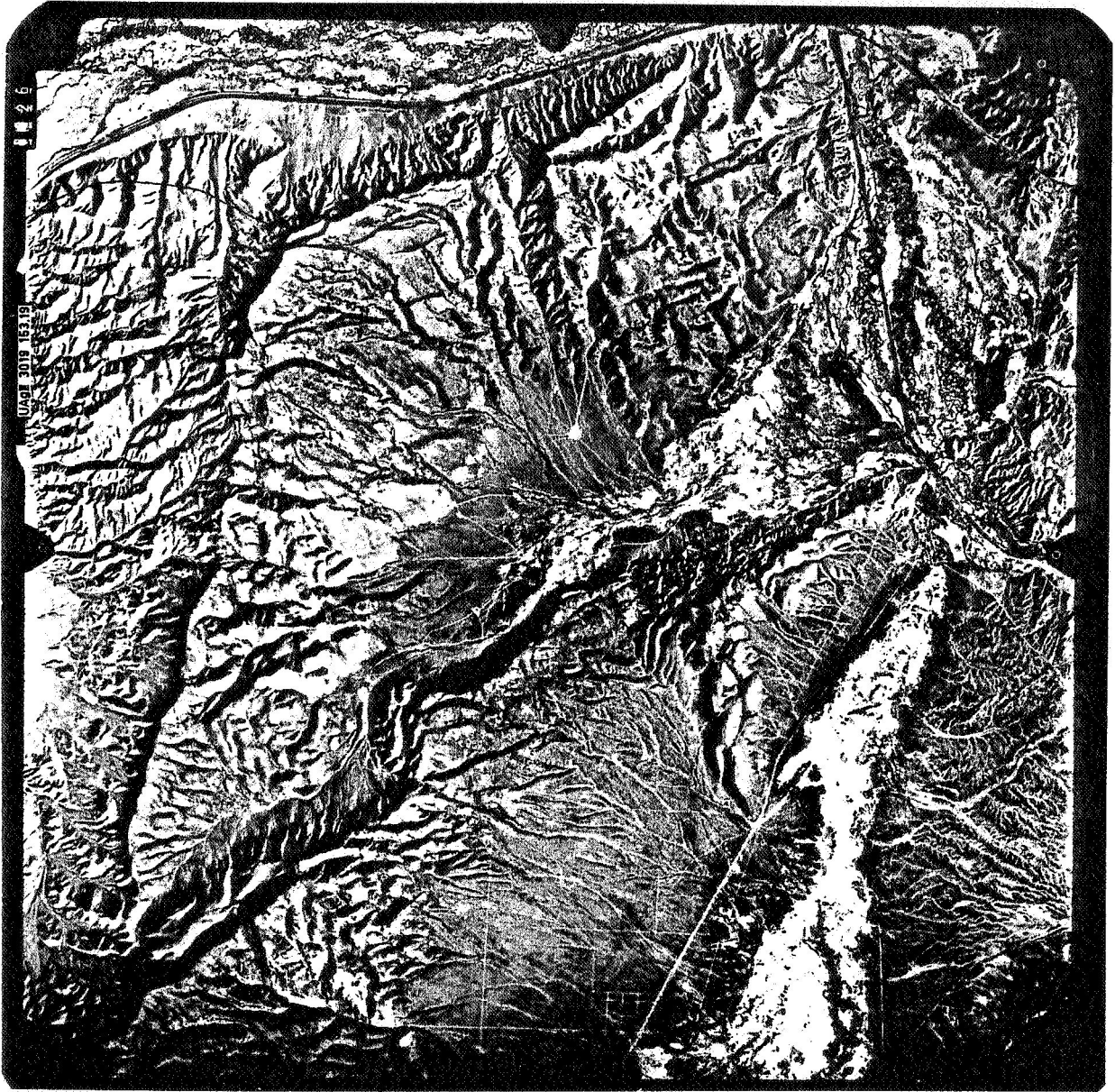


Fig. 3. Vertical aerial photograph of Whirlwind Valley region, Nevada, from 60,000 ft above surface, showing the association of geothermal area (center) near intersection of ENE-trending Malpais escarpment and NNW-trending zone of en-echelon faults. Width of field: approximately 27 km.

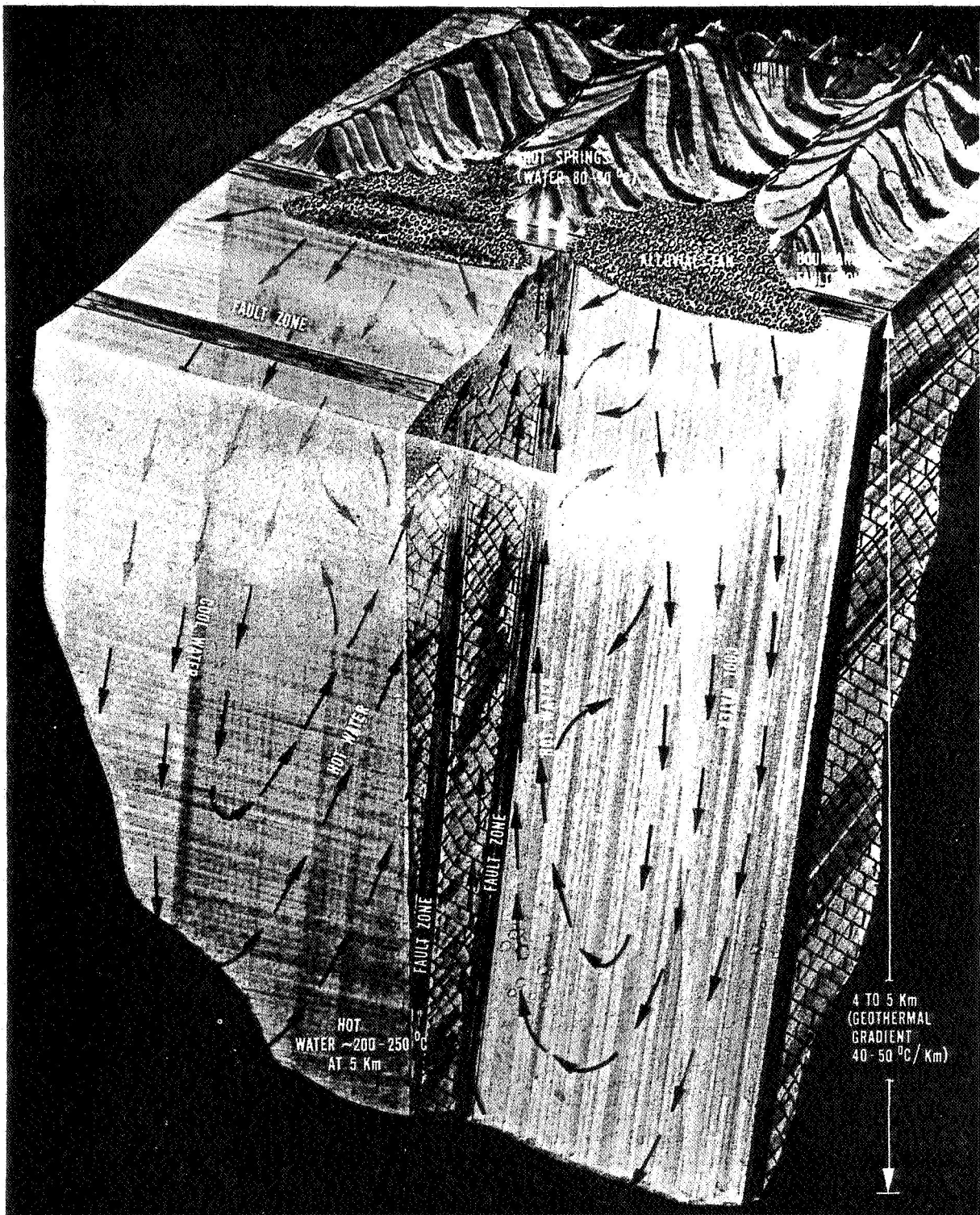


Fig. 4. Schematic cutaway diagram of a geothermal system within a permeable fault zone. Meteoric water enters the fault zone where it intersects near-surface aquifers. Some of the water percolates downward to regions where temperatures reach 150 to 200°C, is heated and rises on the upward limb of a convection cell. Hot springs occur where the cell intersects the surface.

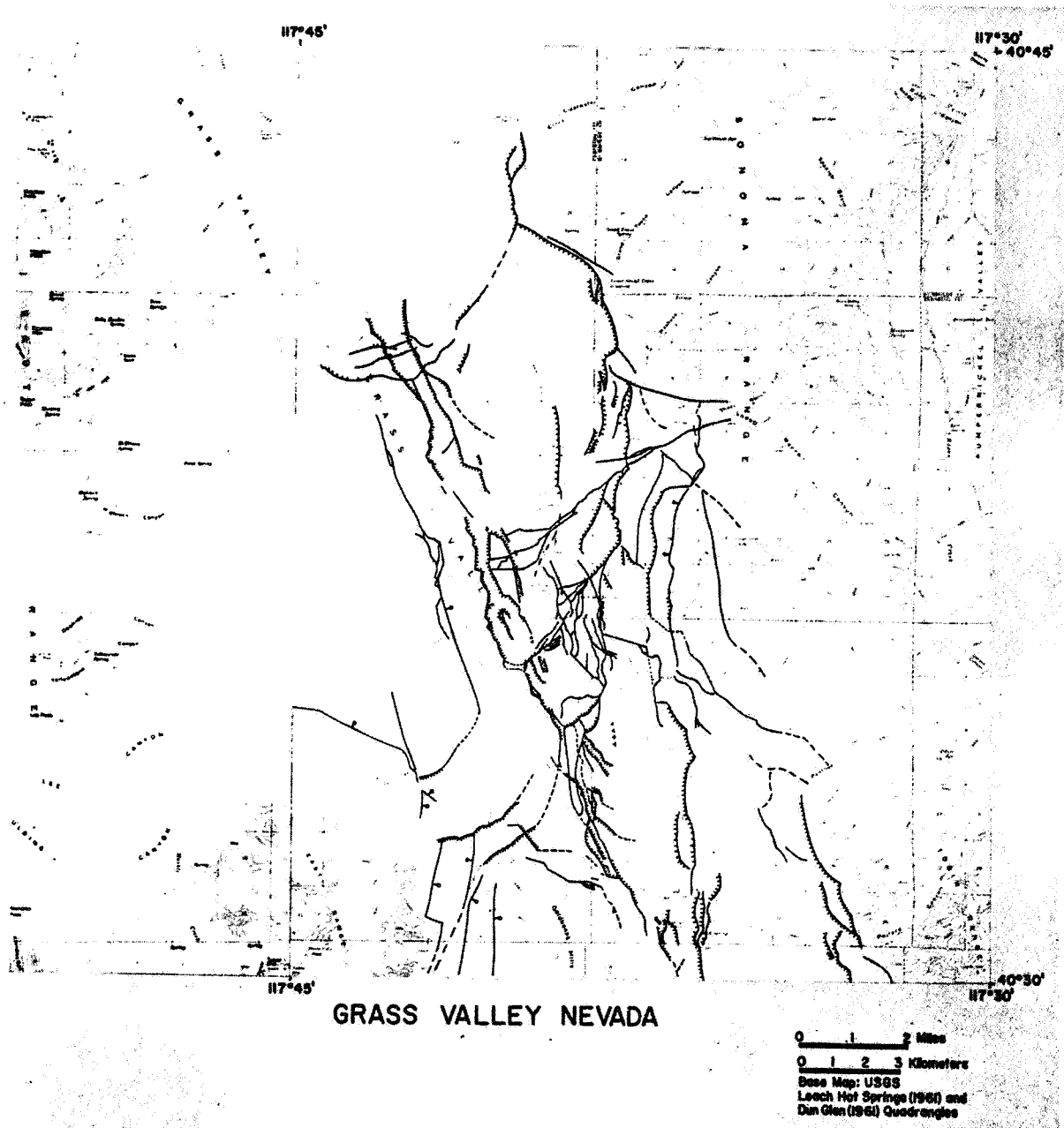


Fig. 5. Fault map of the Leach Hot Springs area. Hachured lines indicate down-faulted sides of scarplets; ball symbol indicates down-thrown side of other faults.

ORIGINAL PAGE IS  
OF POOR QUALITY



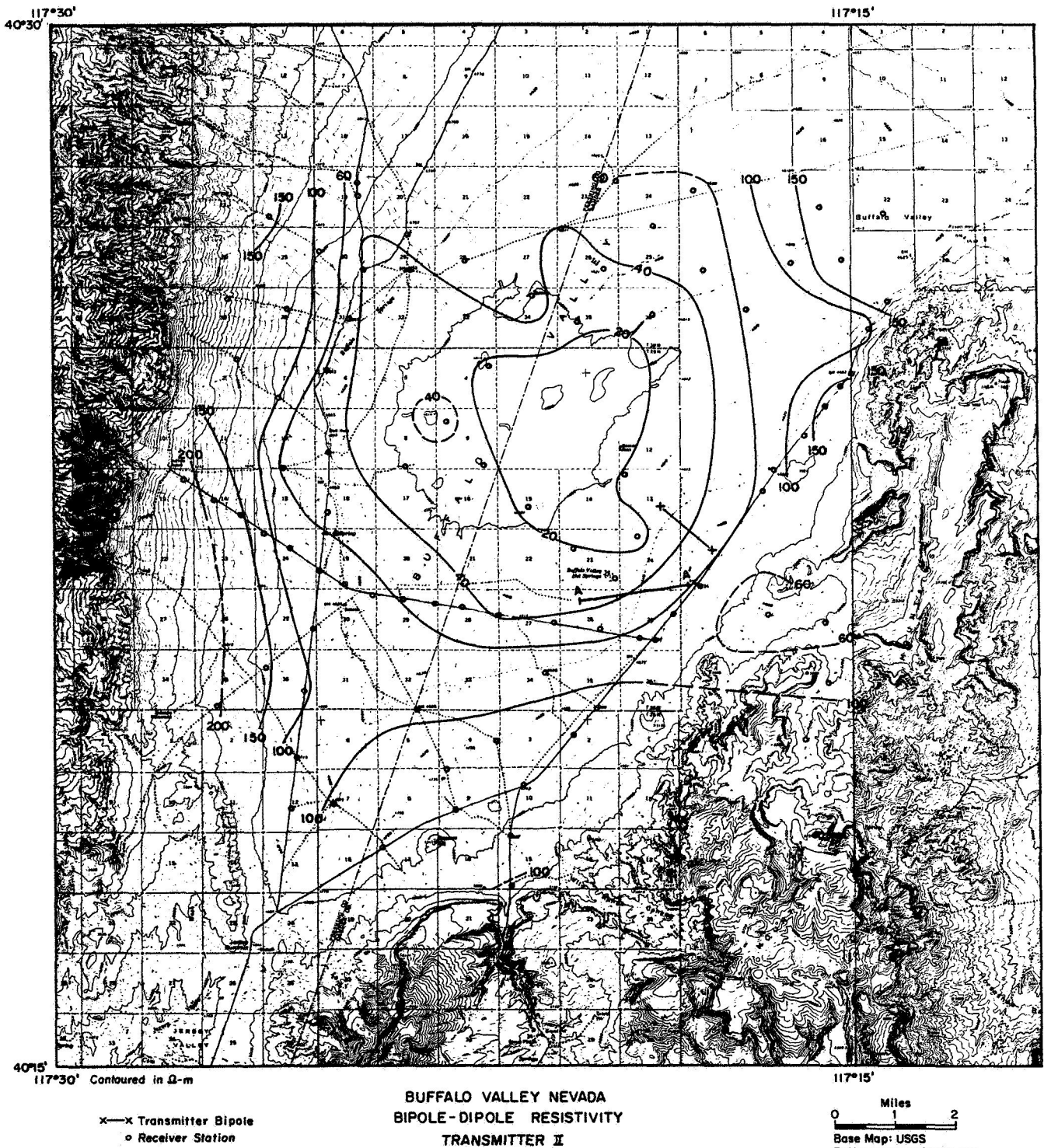


Fig. 6. Apparent resistivity pattern from a bipole-dipole reconnaissance of Buffalo Valley. Current dipole location indicated by heavy line x-x.

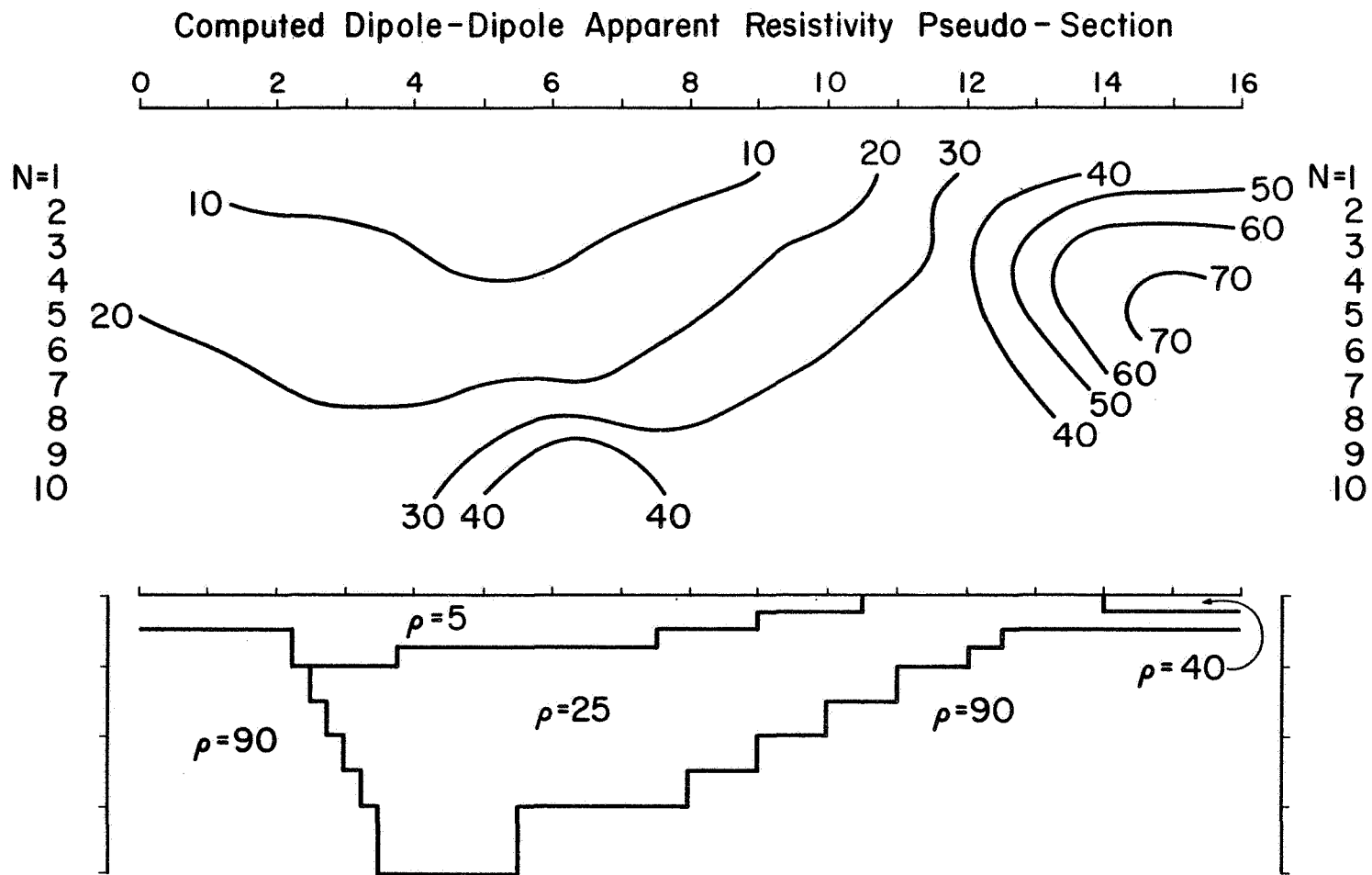


Fig. 7. (upper) Apparent resistivity pseudosection along a profile crossing Buffalo Valley; horizontal distances in km. N-values indicate number of voltage-measurement stepouts from the current dipole, apparent resistivities in ohm-meters. (lower) Computer-generated model based on the pseudosection.

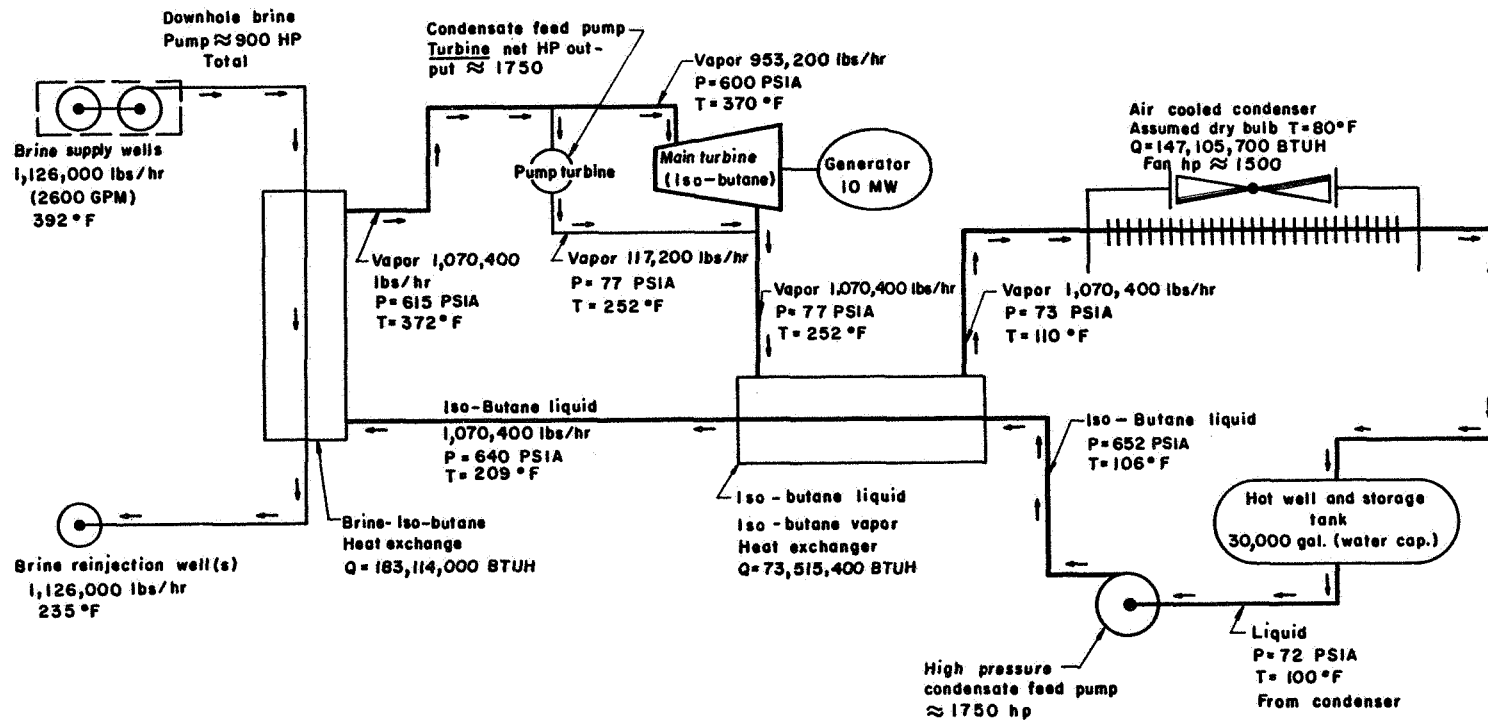
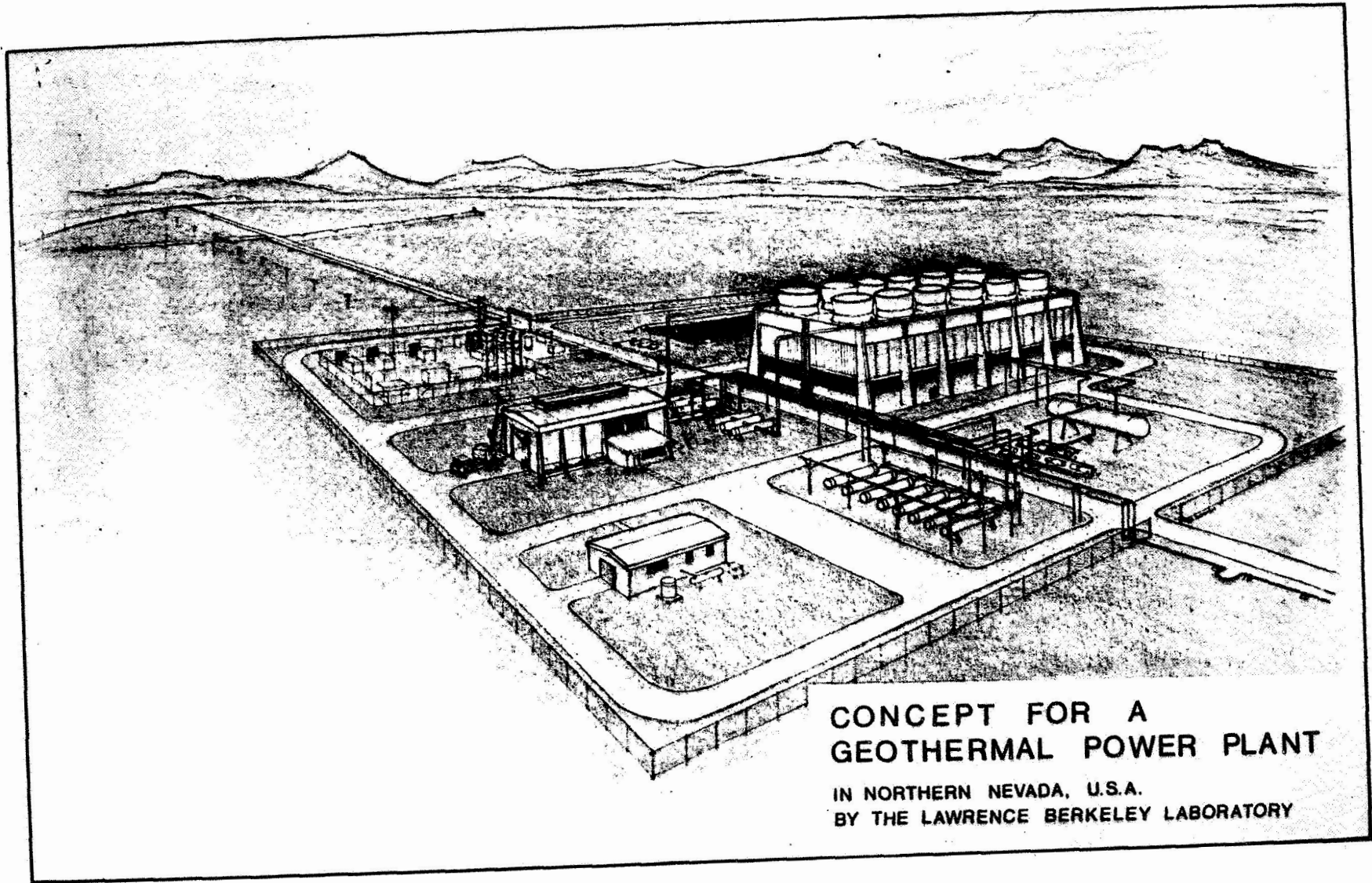


Fig. 8. Simplified flow schematic of 10-MW pilot plant brine and isobutane systems





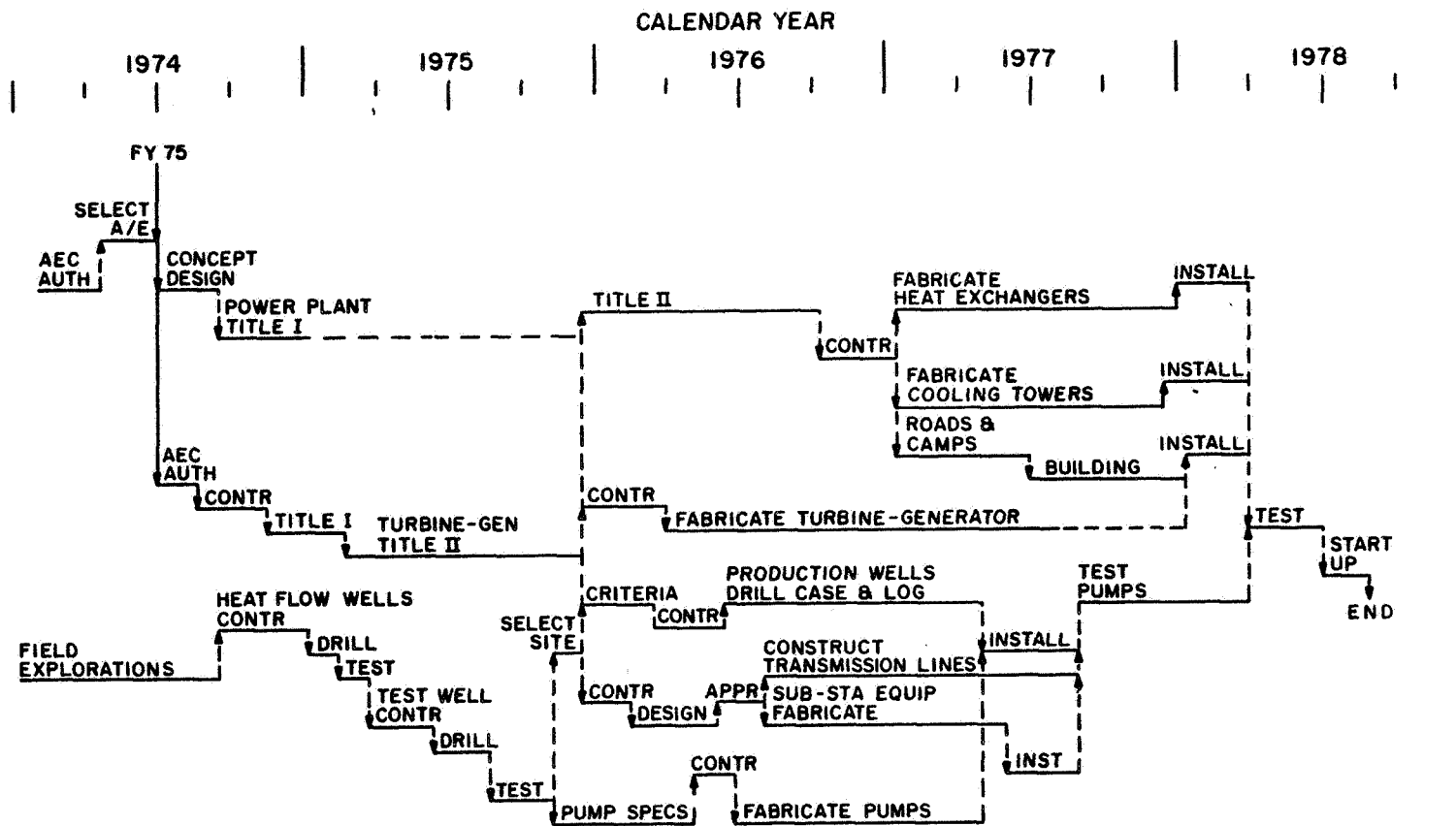
**CONCEPT FOR A  
GEOTHERMAL POWER PLANT**  
IN NORTHERN NEVADA, U.S.A.  
BY THE LAWRENCE BERKELEY LABORATORY

Fig. 9. Pictorial of 10-MW pilot plant

**LBL**  
**GEOTHERMAL FIELD EXPERIMENTAL PLANT**  
**COST ESTIMATE**  
**SUMMARY**

<u>Item</u>	<u>K\$</u>
Brine Distribution	4 50
Isobutane System	2, 7 50
Turbine/Generator	1, 4 85
Cooling Tower	1, 9 70
Electrical Equipment	7 85
General Facilities	3 35
Production/Reinjection Wells	3, 9 75
Engineering	<u>1, 8 25</u>
Subtotal	13, 5 75
Escalation	4, 8 80
Contingency	<u>4, 0 75</u>
<b>TOTAL</b>	<b>K\$ 22, 5 30</b>

Fig. 10. Cost estimate summary for 10-MW pilot plant including production and reinjection wells



GEOHERMAL POWER PLANT -LBL

Fig. 11. 10-MW pilot plant schedule